Draft version March 28, 2017
Preprint typeset using LaTeX style emulateapj v. 12/16/11

A SIMPLE MODEL TO DESCRIBE HOW OUTFLOWS AND ROTATION SHAPE THE LYMAN-α EMISSION LINE IN GALAXIES

Maria Camila Remolina-Gutierrez, Jaime E. Forero-Romero
Departamento de Física, Universidad de los Andes, Cra. 1 No. 18A-10, Edificio Ip, Bogotá, Colombia
Draft version March 28, 2017

ABSTRACT

Young galaxies in the Universe have a strong Ly-α emission caused by the ionized Hydrogen atoms in their interstellar medium. When the spectrum of a galaxy has an intense peak around the Ly-α natural frequency (2.46×10^{15} Hz) it is called a Lyman Alpha Emitter (LAE). Typical LAEs are very distant ($z \gtrsim 2$). This makes that all the data astronomers can obtain from them is their spectra, and from there all the physical information of the galaxy must be derived. Trying to solve this task requires the creation of a simplified and solid model. In this paper we propose to consider LAEs as a spherical distribution of Hydrogen atoms that undergoes a solid body rotation and a radial expansion due to outflows. We use radiative transfer Monte Carlo simulations to interpret the Lyman-α line morphology. The main conclusion is that this new model reproduces LAEs observed features in a clear way and with consistent physical parameters. We also show results of adjusting observational data for some selected objects to models with and without bulk rotation. We finalize by discussing the possible implications for these results in terms of the energetics required for supernova feedback and outflows in high redshift galaxies.

REVISAR AL FINAL...

Subject headings: Galaxies: high-redshift, Lyman Alpha Emission, Galaxy Rotation, Galaxy Outflows, Radiative Transfer

1. INTRODUCTION

Distant galaxies are key to understand early evolutionary stages of our Universe. Physical conditions in those galaxies allows the emergence of Lyman-α line emission at 1216 Å**?**. Galaxies detected through its Lyman-α emission receive the name of spectra at and named Lyman Alpha Emitters (LAEs).

Currently LAEs are commonly targetted in wide area galaxy surveys. They have been effectively used to study galaxy evolution, cosmology and the thermal history of the Universe. This has been able through the study of their spatial distribution and the shape of the Ly-α emission line.

Recent imptovements in instrumentation have revolutionized the kind of studies that can be performed on LAEs. It is now possible to infer detailed kinematic maps for nearby galaxies. The study of these maps would allow us to build data-driven models to interpret the Ly-α spectra of unresolved galaxies, helping us to constrain the physical conditions of the interstellar medium (ISM) processing the Ly-α radiation.

On the ISM's features that plays an important role in shaping the Ly-α is HI kinematics. In a static HI medium the Ly-α line has two equal and symmetric peaks around the natural Ly-α wavelength and zero intensity at the line's center. For an outflowing ISM, the line becomes asymmetrical with a more pronounced read peak. If the galaxy rotates, the line shows different amounts of Doppler shifts modifying the overall line profile Garavito-Camargo et al. (2014).

mc.remolina197@uniandes.edu.co
je.forero@uniandes.edu.co

In this paper we present for the first time a study of the joint effects of galaxy outflows and rotation. We study a simplified geometrical configuration corresponding to an spherical gas cloud with symmetrical radial outflows and a rotation profile corresponding to a solid body.

Djorgovski & Thompson (1992), Rhoads et al. (2000), Gawiser et al. (2007), Koehler et al. (2007), Ouchi et al. (2008), Yamada et al. (2012), Schenker et al. (2012), Kulas et al. (2012), Yamada et al. (2012), Chonis et al. (2013), Finkelstein et al. (2013), Östlin et al. (2014), Hayes et al. (2014), Faisst et al. (2014), Fumagalli et al. (2015).

Our main goal with this work is to measure the effect of the model's physical parameters on the outgoing Ly-α line. In this case, due to the resonant[1] nature of the Ly-α line, analytical solutions can not be derived. Because of this, it becomes necessary to run simulations that explore and test the model. In this paper we use the radiative transfer code **CLARA** (Code for Lyman Alpha Radiation Analysis) written by Forero-Romero et al. Forero-Romero et al. (2011). CLARA can simulate the Ly-α line of a spherical rotating LAE depending on its mass and velocity, so we modify it to include outflows and then we explore the resulting consequences on the Ly-α line.

2. A NEW LAE MODEL

We model spherical galaxy to facilitate the interpretation of the results, by deleting what would be another

[1] Resonant is a common term used in radiative transfer. It means that the photons that create the line are absorbed and re-emitted several times before escaping the cloud of gas.

degree of freedom regarding a different geometry. Furthermore, this approximation is commonly used in the literature, as it explains a wide variety of observational features (Ahn et al. (2003), Verhamme et al. (2006), Dijkstra et al. (2006)).

There are 3 parameters in this model that define a LAE: the rotational velocity ($v_{\rm rot}$), the outflow velocity ($v_{\rm out}$) and the optical depth ($\tau_{\rm H}$). $v_{\rm out}$ is due to material ejected from the galaxy, by supernovas(Verhamme et al. (2006), Orsi et al. (2012), Hashimoto et al. (2015), Gronke et al. (2015)). $\tau_{\rm H}$ roughly corresponds to number of H atoms found by a Ly-α photon if one traces a line from the center of the galaxy to its edge, and it resembles the mass of the LAE.

In this model, the LAE has a bulk velocity corresponding to the superposition of rotation and outflows, as shown in Fig. 1. The velocity components are written in Eqs. (1) (2) (3). In these equations, R is the radius of the sphere; x, y and z are the coordinates in a cartesian frame; and the $\mp$ signs in v_x and v_y indicate the direction of rotation, respectively. This rotation is a solid body rotation and its direction goes according to the right hand rule applied to the $\hat{k}$ unit vector. The outflow velocity is dependent on the position relative to the center of the galaxy, being it zero at the center and maximum at the edge of the sphere.

$$v_x = \frac{x}{R}v_{\rm out} - \frac{y}{R}v_{\rm rot} \quad (1)$$

$$v_y = \frac{y}{R}v_{\rm out} + \frac{x}{R}v_{\rm rot} \quad (2)$$

$$v_z = \frac{z}{R}v_{\rm out} \quad (3)$$

These 3 parameters, $v_{\rm rot}$, $v_{\rm out}$ and $\tau_{\rm H}$, leave the idea of a model of LAE, that although simple, considers the main galaxy's dynamics. All of them have been previously proposed and used by different authors, but never combined together (Adams (1972), Harrington (1973), Neufeld (1990), Dijkstra et al. (2006), Verhamme et al. (2006), Forero-Romero et al. (2012), Martin et al. (2015), Garavito-Camargo et al. (2014), Neufeld (1991), Laursen et al. (2009), Barnes et al. (2011), Verhamme et al. (2012), Yajima et al. (2012)).

However, in the plots shown in this paper we use instead velocity, V, units. This eases the comparison against observational data. The velocity units are defined by The units of V are usually km s^{-1}. In this case, the photon is redshifted in frequency when the velocity is greater than 0, and blueshifted in the opposite case.

The initial emission of photons is taken at the center of the sphere for practicality due to the fact that both, center and off-center emissions, give analogous results. From here, 100000 photons are emitted with the natural Ly-α wavelength and start to scatter. When each photon is re-emitted, its new wavelength depends on the H atom's velocity (both thermal and bulk) and direction (both initial and final). However the photon's new direction of propagation is random in the rest frame of the atom.

The individual scattering of all the photons is tracked through the complete 3D Hydrogen distribution. Once each photon escapes the galaxy, its final values are stored: position $\vec{r}$, direction of propagation $\hat{k}$, dimensionless frequency x, and number of scatterings N. To build the observed spectrum we make a histogram of the escape frequencies x. The number of scatterings N tells how many steps the random walk requires to reach a distance to the center that is $\geq R$. In order to avoid situations in which the photon has not escaped after a long computational time, CLARA defines a number N_{max} so the code stops. However, according to statistics, this last situation has low probabilities, so the photon is always most likely to exit the sphere.

2.1. *Galaxy's Viewing Angle*

An observer located far away, only receives photons emitted along its line of sight. That means, only photons escaping in the direction of the observer must be counted in the spectrum. In the simulation we approximate this by taking into account only the photons with escaping direction angle θ respect to the rotation axis within the range $[\theta_{min} - \theta_{max}]$. We illustrate this in Fig. 1.

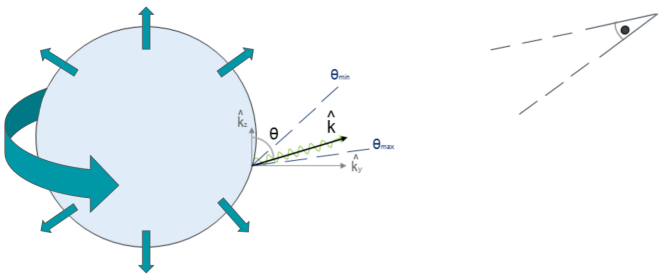

FIG. 1.— **Model:** Spherical LAE with tangential and radial velocities due to rotation and outflows, respectively. The galaxy cut is in the $y-z$ plane perspective. The observer is located at an specific viewing angle of the sphere. Only photons with a direction that enters in this range of vision are taken into account to build the observed spectrum.

Therefore, in principle the spectra depend on two new parameters, the azimuthal and the polar angle. However, the galaxy's motion is symmetrical respect to its rotation axis. This implies that the resulting spectrum is independent from the azimuthal angle. Taking into account this symmetry, we only select photons on their polar angle, regardless of their azimuthal angle. Regarding the polar angle, we build the spectra for observers located on 3 different positions, with θ intervals uniformly distributed in $\cos(\theta)$.

To summarize, the parameters influencing the spectra are $v_{\rm rot}$, $v_{\rm out}$, $\tau_{\rm H}$ and θ. In the next section we evaluate the impact each of these has on the resulting profile.

3. RESULTS

3.1. *Resulting simulated spectra*

In order to define the ranges of $\tau_{\rm H}$, $v_{\rm rot}$ and $v_{\rm out}$, it is necessary to refer to observational constraints. The common values for typical LAEs that were set as parameters are in Tab. 1. We run CLARA's modified version for all the permutations of these 3 parameters.

$\tau_{\rm H}$	v_{rot} (km s^{-1})	v_{out} (km s^{-1})
10^5, 10^6, 10^7	50, 100	5, 10, 15, 20, 25, 50, 75

TABLE 1
Parameters' Values: All consistent with a LAE's typical properties

The behavior of the resulting sets of spectra can be summarized by Fig. 2. We concluded from the simulations a clear creation of two asymmetric peaks around $V = 0$ km s^{-1}with the tallest peak always redshifted. We detected a strong dependence on the outflow velocity that induces the peak asymmetry. We also detected that the rotation velocity broadens the line horizontally. Both these effects have been previously reported separately in the literature, so these results can valid their superposition to some extend.

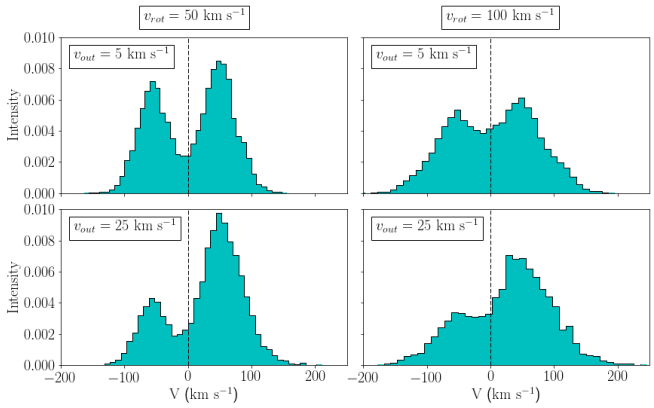

FIG. 2.— **4 different Ly-α profiles:** With $\tau_{\rm H} = 10^5$ and $\theta \simeq 90°$. The rotational velocity $v_{\rm rot}$ increases to the right and the outflows velocity $v_{\rm out}$ increases downwards. The intensity is in arbitrary units.

3.2. *Influence of the viewing angle θ*

We take now into account the viewing angle of the galaxy to build the observed spectra. For all of the physical parameters' combinations, the effect of θ in the Ly-α line is always the same.

From Fig. 3 it is clear that the intensity of the valley between the two peaks increases along with θ. This causes an intensity decrease in the rest of the frequencies, thus a broadening of the line. The asymmetry also changes with the viewing angle.

3.3. *Morphology of Ly-α line*

To summarize, the influence of the 4 parameters on the Ly-α morphology is the following:

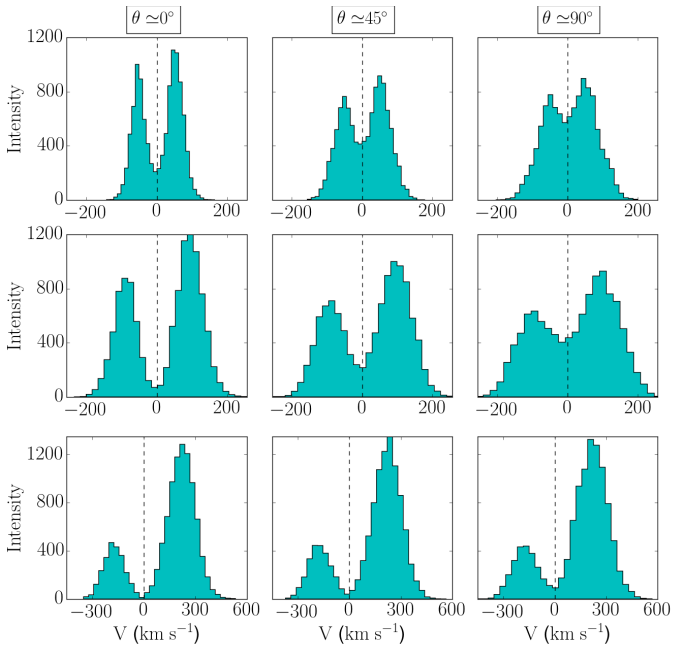

FIG. 3.— **Ly-α profile for different θ.** For $\tau_{\rm H} = 10^5$, $v_{\rm rot} = 50$ km s^{-1}and $v_{\rm out} = 20$ km s^{-1}. For $\tau_{\rm H} = 10^6$, $v_{\rm rot} = 100$ km s^{-1}and $v_{\rm out} = 5$ km s^{-1}. For $\tau_{\rm H} = 10^7$, $v_{\rm rot} = 100$ km s^{-1}and $v_{\rm out} = 15$ km s^{-1}. The intensity is in arbitrary units.

- $\tau_{\rm H}$ induces a redshift. Increasing the optical depth separates the line of the zero velocity line.
- $v_{\rm out}$ decreases the right peak's intensity. Higher $v_{\rm out}$ makes the left peak smaller until it merges with the right one.
- $v_{\rm rot}$ broadens the line and decreases the maximum intensity. Higher $v_{\rm rot}$ implies a flatter spectrum. This effect has not been deeply studied in literature. Only Garavito et al. Garavito-Camargo et al. (2014) has simulated its effect. Our results are consistent with their conclusions.
- θ increases the central valley of the line. Higher θ makes more emission at Ly-α natural frequency.

3.4. *Doppler shift by rotation*

The rotation effect induces a Doppler shift in frequency and displaces the only-outflow spectra. As seen in Fig. 4 rotation takes the resulting spectrum with $v_{\rm rot} = 0$ and displaces it from its central location. Then it weights the lines and they all merge into the resulting red Ly-α line.

PONER GRAFICA REAL...

4. OBSERVATIONAL IMPLICATIONS

Among the observational implications that this paper has over observations we select three principal ones. First, the rotational effects of the galaxy should be clearly detected and characterized by MUSE's high

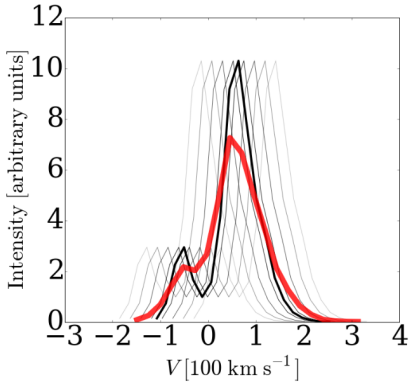

FIG. 4.— **Rotations induces a Doppler shift of the only-outflow spectra:** Each of the black lines is then weighted to obtain the red line.

resolution data. The Doppler redshift is already visible in other observations, such as the one seen in Fig. 7 of Prescott et al. Prescott et al. (2015).

Second, the central ($V = 0$) emission of the spectra seen in the results is a consequence of the viewing angle of the galaxy and can be controlled by it. This means that the reason is not necessary that radiation is escaping without scattering, as several authors have suggested (CITAS...).

Finally, all the spectra produced from this new LAE model is roughly consistent with observations. The consideration of adding the new rotation parameter to the standard only-outflow model found in literature is reasonable and very powerful. $v_{\rm rot}$ and its consequent viewing angle θ can modify the morphology of the Ly-α line in new different ways by keeping the model simplified.

5. CONCLUSIONS

In this paper, the objective was to analyze and measure the influence of galaxy rotation and outflows on the Ly-α line. The motivation for this is to be able to obtain physical information of a LAE by just looking at its Ly-α profile. In order to accomplish this objective, we propose a new model of a LAE consisting of a sphere of Hydrogen atoms that expands radially and rotates as a solid body. A modified version of the program CLARA Forero-Romero et al. (2011) is used to set the conditions and emulate the radiative transfer process inside the galaxy.

The conclusions obtained from this work are:

- The outgoing spectra depend on the angle an external observer is viewing the galaxy from. The closer it is to the equator of the galaxy, the higher the central valley of the frequency distribution.
- The effects of $v_{\rm rot}$, $v_{\rm out}$ and $\tau_{\rm H}$ are consistent with the different authors that have used them. $v_{\rm rot}$ broadens the Ly-α line. $v_{\rm out}$ increases the peaks asymmetry and $\tau_{\rm H}$ induces a redshift around the zero velocity.
- Rotations induces a Doppler shift in frequency of the only-outflow spectra.
- The final spectra obtained are roughly consistent with LAEs observations.

5.1. *Future work*

For future work regarding the model, we would like to implement a differential rotation for the LAE instead of solid body. Regarding result analysis, we would like to compare against observations in two ways. Firstly by using the kinematic observation obtained from newly observed LAEs. We could do a consistency check between their real spectra and the simulated one that our model would produce with the respective parameters. Secondly we would like to take a specific observed spectrum and fit it using MCMC in order to predict ranges for its parameters.

5.2. *Reproducibility*

All of this work is available online and free to use to anyone. The data, source code and instructions to replicate this paper's results are in the GitHub repository: `github.com/astroandes/CLARA_RotationOutflows`.

ACKNOWLEDGMENTS

The authors would like to acknowledge the high performance computational cluster (HPC) hosted by Universidad de los Andes, where we ran the simulations for CLARA.

We would also like to acknowledge the participants of the meeting *Escape of Lyman radiation from galactic labyrinths* at Crete, Greece, for their valuable comments on this work, specially to Max Gronke and Christian Herenz.

REFERENCES

Adams, T. F. 1972, ApJ, 174, 439
Ahn, S.-H., Lee, H.-W., & Lee, H. M. 2003, MNRAS, 340, 863
Barnes, L. A., Haehnelt, M. G., Tescari, E., & Viel, M. 2011, MNRAS, 416, 1723
Chonis, T. S., Blanc, G. A., Hill, G. J., Adams, J. J., Finkelstein, S. L., Gebhardt, K., Kollmeier, J. A., Ciardullo, R., Drory, N., Gronwall, C., Hagen, A., Overzier, R. A., Song, M., & Zeimann, G. R. 2013, ApJ, 775, 99
Dijkstra, M., Haiman, Z., & Spaans, M. 2006, ApJ, 649, 14
Djorgovski, S., & Thompson, D. J. 1992, in IAU Symposium, Vol. 149, The Stellar Populations of Galaxies, ed. B. Barbuy & A. Renzini, 337
Faisst, A. L., Capak, P., Carollo, C. M., Scarlata, C., & Scoville, N. 2014, ApJ, 788, 87

Finkelstein, S. L., Papovich, C., Dickinson, M., Song, M., Tilvi, V., Koekemoer, a. M., Finkelstein, K. D., Mobasher, B., Ferguson, H. C., Giavalisco, M., Reddy, N., Ashby, M. L. N., Dekel, a., Fazio, G. G., Fontana, a., Grogin, N. a., Huang, J.-S., Kocevski, D., Rafelski, M., Weiner, B. J., & Willner, S. P. 2013, Nature, 502, 524
Forero-Romero, J. E., Yepes, G., Gottlöber, S., Knollmann, S. R., Cuesta, A. J., & Prada, F. 2011, MNRAS, 415, 3666
Forero-Romero, J. E., Yepes, G., Gottlöber, S., & Prada, F. 2012, MNRAS, 419, 952
Fumagalli, M., O'Meara, J. M., Prochaska, J. X., Rafelski, M., & Kanekar, N. 2015, MNRAS, 446, 3178
Garavito-Camargo, J. N., Forero-Romero, J. E., & Dijkstra, M. 2014, ApJ, 795, 120
Gawiser, E., Francke, H., Lai, K., Schawinski, K., Gronwall, C., Ciardullo, R., Quadri, R., Orsi, A., Barrientos, L. F., Blanc, G. A., Fazio, G., & Feldmeier, J. J. 2007, ApJ, 671, 278
Gronke, M., Bull, P., & Dijkstra, M. 2015, ApJ, 812, 123
Harrington, J. P. 1973, MNRAS, 162, 43
Hashimoto, T., Verhamme, A., Ouchi, M., Shimasaku, K., Schaerer, D., Nakajima, K., Shibuya, T., Rauch, M., Ono, Y., & Goto, R. 2015, ApJ, 812, 157
Hayes, M., Östlin, G., Duval, F., Sandberg, A., Guaita, L., Melinder, J., Adamo, A., Schaerer, D., Verhamme, A., Orlitová, I., Mas-Hesse, J. M., Cannon, J. M., Atek, H., Kunth, D., Laursen, P., Otí-Floranes, H., Pardy, S., Rivera-Thorsen, T., & Herenz, E. C. 2014, ApJ, 782, 6
Koehler, R. S., Schuecker, P., & Gebhardt, K. 2007, A&A, 462, 7
Kulas, K. R., Shapley, A. E., Kollmeier, J. A., Zheng, Z., Steidel, C. C., & Hainline, K. N. 2012, ApJ, 745, 33
Laursen, P., Sommer-Larsen, J., & Andersen, A. C. 2009, ApJ, 704, 1640
Martin, C. L., Dijkstra, M., Henry, A., Soto, K. T., Danforth, C. W., & Wong, J. 2015, ApJ, 803, 6
Neufeld, D. A. 1990, ApJ, 350, 216
—. 1991, ApJl, 370, L85
Orsi, A., Lacey, C. G., & Baugh, C. M. 2012, MNRAS, 425, 87
Östlin, G., Hayes, M., Duval, F., Sandberg, A., Rivera-Thorsen, T., Marquart, T., Orlitova, I., Adamo, A., Melinder, J., Guaita, L., Atek, H., Cannon, J. M., Gruyters, P., Herenz, E. C., Kunth, D., Laursen, P., Mas-Hesse, J. M., Micheva, G., Pardy, H. O.-F. S. A., Roth, M. M., Schaerer, D., & Verhamme, A. 2014, ArXiv e-prints
Ouchi, M., Shimasaku, K., Akiyama, M., Simpson, C., Saito, T., Ueda, Y., Furusawa, H., Sekiguchi, K., Yamada, T., Kodama, T., Kashikawa, N., Okamura, S., Iye, M., Takata, T., Yoshida, M., & Yoshida, M. 2008, ApJs, 176, 301
Prescott, M. K. M., Martin, C. L., & Dey, A. 2015, ApJ, 799, 62
Rhoads, J. E., Malhotra, S., Dey, A., Stern, D., Spinrad, H., & Jannuzi, B. T. 2000, ApJl, 545, L85
Schenker, M. A., Stark, D. P., Ellis, R. S., Robertson, B. E., Dunlop, J. S., McLure, R. J., Kneib, J.-P., & Richard, J. 2012, ApJ, 744, 179
Verhamme, A., Dubois, Y., Blaizot, J., Garel, T., Bacon, R., Devriendt, J., Guiderdoni, B., & Slyz, A. 2012, A&A, 546, A111
Verhamme, A., Schaerer, D., & Maselli, A. 2006, A&A, 460, 397
Yajima, H., Li, Y., Zhu, Q., Abel, T., Gronwall, C., & Ciardullo, R. 2012, ApJ, 754, 118
Yamada, T., Nakamura, Y., Matsuda, Y., Hayashino, T., Yamauchi, R., Morimoto, N., Kousai, K., & Umemura, M. 2012, AJ, 143, 79